Electrothermal Icing Protection of Aerosurfaces Using Conductive Polymer Nanocomposites

Samuel T. Buschhorn[1], Noa Lachman[3], Jennifer Gavin[4], and Brian L. Wardle[6]
Massachusetts Institute of Technology, Cambridge, MA, 02139

Seth S. Kessler[2], Greg Thomas[5]
Metis Design Corporation, Boston, MA, 02114

Ice protection systems (IPS) are critical components for many aerospace flight vehicles, including commercial transports and unmanned aerial systems (UAS), and can include anti-icing, de-icing, ice sensing, etc.. Here, an IPS is created using nanomaterials to create a surface-modified external layer on an aerosurface based on observations that polymer nanocomposites have tailorable and attractive heating properties. The IPS uses Joule heating of aligned carbon nanotube (CNT) arrays to create highly efficient de-icing and anti-icing of aerosurfaces. An ice wind tunnel test of a CNT enhanced aerosurface is performed to demonstrate the system under a range of operating regimes (temperature, wind speed, water content in air) including operation down to -20.6°*C* (-5°*F*) at 55.9 *m/s* (125 *mph*) under heavy icing. Manufacturing, design considerations, and further improvements to the materials and systems are discussed.

I. Introduction

ICE formation on aerosurfaces has a number of detrimental effects impacting economical, safe and weather-independent operation of aircraft. A wide range of technologies have emerged to address the issue over time. Even though some technologies have been refined over the course of more than 70 years, with considerable innovation and new technologies being adopted, only a few were certified and see use on a meaningful commercial scale. Implementation was hindered by drawbacks such as added weight, power consumption, maintenance requirements, negative impact on (long term) structural properties, and design integration issues. This is especially true for high performance applications, which typically use advanced materials such as fiber reinforced plastic (FRP) advanced composites. Often IPS' requires utilization of materials in auxiliary systems that, at minimum, perform equally well for either mechanical or environmental stresses. Carbon nanotubes (CNTs) are a promising material for improving mechanical[1,] and multifunctional properties[2] of FRP composites in nanoengineered composite architectures, and they are explored here for use as an IPS.

Some of the traditional approaches used to deal with ice accretion include "weeping wing" freezing point depressors, pneumatic systems with a flexible leading edge, hot gas systems, or electrothermal systems. In recent years a number of new approaches were developed[3,4]. In terms of electrothermal technologies, developments that use largely conventional materials are already yielding significant improvements[5,6]. These merits can be exploited even more thoroughly if advanced nanoscale materials, such as CNTs, bring their exceptional qualities to bear[7]. Due to their small size they can be seamlessly integrated while maintaining or enhancing structural properties, or surface finish. Previous studies report significant improvements of mechanical properties[8,9] using vertically-aligned CNT arrays with effectively no increase in weight or volume. Aligned-CNT based "nanostitching" of interlaminar regions

[1] Postdoctoral Associate, Department of Aeronautics and Astronautics, 77 Massachusetts Ave, Bldg. 41-317.
[2] President, Metis Design Corporation, 205 Portland St.
[3] Postdoctoral Associate, Department of Aeronautics and Astronautics, 77 Massachusetts Ave, Bldg. 41-317.
[4] Visiting Undergraduate Student, Department of Materials Science and Engineering, 77 Massachusetts Ave. Dept. of Mechanical Engineering, 2525 Pottsdamer St, Florida State University, Tallahassee, FL, 32310.
[5] Propulsion Engineer, Metis Design Corporation, 205 Portland St.
[6] Associate Professor, Department of Aeronautics and Astronautics, 77 Massachusetts Ave, AIAA Associate Fellow.

can easily be combined with other deicing technologies, since CNTs are generally not negatively affected through moderate deformation, small discontinuities, strong electromagnetic fields, or high current densities. Such aligned CNTs can also be integrated into the surface of a FRP composite, or even into an epoxy film on the surface of the composite as used here. In this way, a solution can be designed to maximize efficiency of intermittent or continuous operation by locating and integrating the deicing layer extremely close to the ice/airfoil interface. Due to the extremely high maximum current density, low heat capacity, high thermal conductivity, and a uniform (or tailored) resistance distribution of CNTs, a dynamic operation for the IPS is envisioned. This would enable a secondary problem of de-icing to be addressed, which concerns how and where the ice is shed. Especially for rotating aerosurfaces, such as wind power rotor blades, helicopter rotor blades, or even open prop fan blades, a fast reaction, high performance, high fidelity IPS could enable more economical operation and designs.
This report treats design considerations, the manufacture and assembly of a prototype CNT based electrothermal anti-icing and de-icing device, and subsequent testing of a large-scale (m-scale) aerosurface in an ice wind tunnel.

II. Design Considerations

An initial model of atmospheric conditions, aerodynamics, and thermal flux was made to assess approximate system requirements. The main goal was to enable the determination of key parameters that the CNT IPS should possess in order to work with a given power supply for a specific area and position on the airfoil. This resulted in a range and layout of electrical resistivities that would dissipate the electrical power in the form of heat, as necessary for effective anti-icing or de-icing. The IPS uses Joule heating, and the necessary electrical resistance can be expressed in terms of Ohms per square, and was calculated via coupled thermofluid models to derive the heating required for both de-icing and anti-icing. Nanostitch (vertically-aligned CNTs, VACNTs, in polymer) sheet resistance values were measured and sheet resistance tailored by controlling the morphology of the aligned CNTs in the polymer, thereby enabling the fabrication of required resistivities that vary spatially over the aerosurface.

This approach allows using several degrees of freedom to vary in order to attain one specific electrical sheet resistance (or more precisely: electrical resistance tensor). These properties originate from complex structure-property-relationships at various scales. Perhaps the most fundamental parameter relates to the individual CNT morphology, which is of a specific crystallographic structure (known as chirality) resulting in three distinct electrical property profiles. However, influencing the chirality distribution of CNTs at a large scale (~10-100 Billion CNTs – cm^{-1}) is not yet practical, so a homogenized material can be assumed at the macroscopic scale.

The next aspect of morphology is defined through the length of the individual CNTs. In the CVD process used in this study there is a fairly simple relation between duration of synthesis (growth time) and forest height, which is plotted in Fig. 1. This characteristic of the material can be easily and reliably manipulated, and was therefore chosen as a primary factor for adjusting the sheet resistance of the heating layer. The material was only taken from the positions in the furnace that would produce forests of approximately the same height in order to avoid large deviations of sheet resistance.
On a microscopic level, the resistance and heating in a CNT array remains unevenly distributed, and is strongly dependent on the current flow direction. For an as-grown array or forest, the resistance is significantly lower along the principal axis of the CNTs than perpendicular to it. It is obvious that the conductivity parallel to the CNT primary axis correlates relatively closely with the sheet resistance in this direction. Also, the sheet resistance is strongly influenced by the electrical contacts between adjacent CNTs[10,11]. The number and nature of these contacts depends on the length, spacing, waviness, and diameter of the CNTs and does not necessarily follow a strict linear relationship that is implied by a conductivity value. While previous studies have begun to quantify and model these morphology effects[12,13], implementing these models to such as system will be the subject of future investigations, and is not within the scope of this paper. It should only be noted as these aspects represent further degrees of freedom that could be used to control the current flow and heat dissipation in the IPS material.

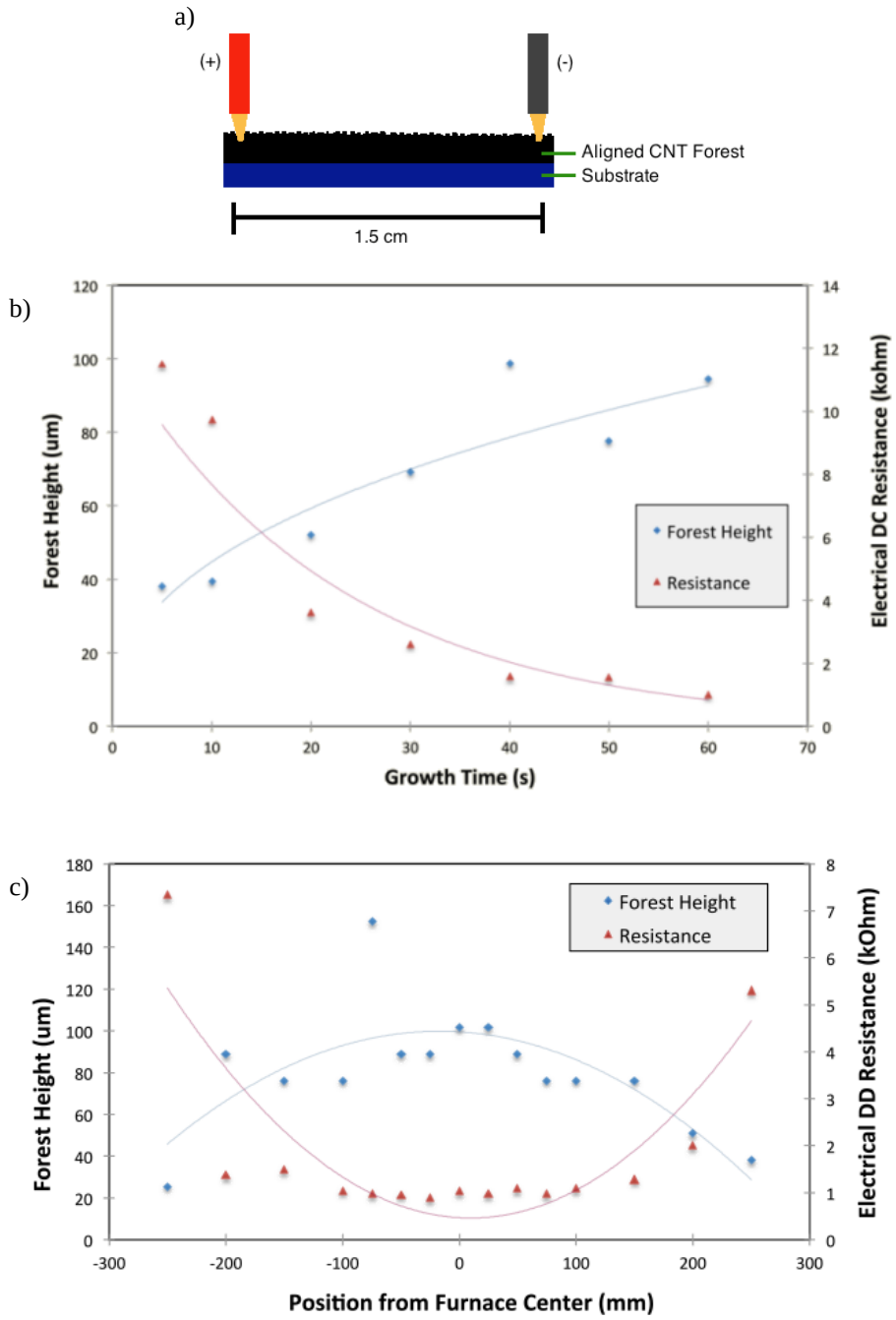

Fig. 1: Aligned-CNT properties used in IPS: a) Schematic of 2-point resistance measurement performed on the CNT forests, using a digital multimeter and spring loaded gold plated contact pins for electrodes, b) CNT forest height at the furnace center for different synthesis times, and the corresponding electrical resistance as measured with a digital multimeter, and c) Different CNT forest growth heights at a range of locations in the furnace for a growth time of 60 *s*, the growth duration used here for the IPS.

For the manufacturing of the resistive heating layer, it was decided to modify the CNT morphology by pushing them over (see Figure 3 a-c), and compressing them at the same time. This is sometimes called "knock-down" or "vertical densification", and can be performed in a variety of similar ways[14-18]. The knocked down and compacted CNT layer becomes more mechanically robust than the as-grown CNT arrays (used as nanostitches). Due to the

increased CNT volume fraction, there are many more parallel electrical contacts, which result in a more consistent and lower overall sheet resistance.

Before production of the airfoil heating device began, a number of smaller samples were produced to determine CNT length, quality, and test viability of different microstructural modifications and contacting methods. Figure 2 a) shows some samples produced to determine local and directional variation of electrical resistance. The directional nature of the electrical resistance could be influenced through tailoring the CNT array morphology during and after growth, and allows modifying the electrical current distribution for the IPS. In the manufacturing of the prototype heating device, however, it was not necessary to exploit this option. Figure 2 b) shows a thermal image of a sample produced to assure good electrical current distribution using a rivet based wiring connection on a glass fiber reinforced plastic (GFRP) composite substrate.

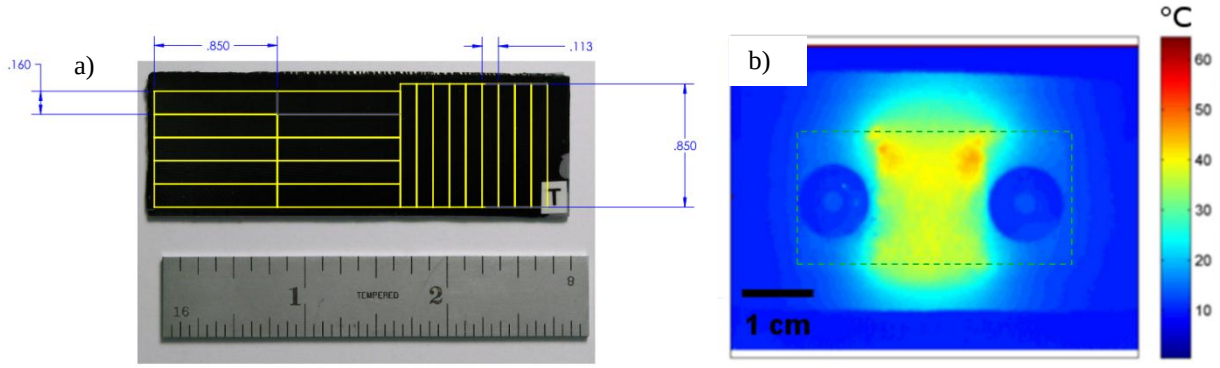

Fig. 2: Polymer nanocomposite IPS preliminary testing: a) knockdown aligned CNT layer cured on an epoxy film adhered to a glass slide. The rectangular delineations indicate individual electrical-resistance test samples. These samples were contacted at the side faces with silver paint and characterized using a digital multi-meter, and b) A low power experiment shows heat distribution across an aligned CNT layer (dashed rectangle) in an epoxy film mounted on a glass fiber reinforced plastic composite sample. The dark round shapes represent rivets, with their centers approx. 30 *mm* apart, that served as electrical contacts.

III. Nanostitch IPS Fabrication

Aligned CNT forests were produced in a modified chemical vapor deposition process[19]. From the aforementioned experiments it could be determined that a modification of growth time and shear compaction, as seen in Figure 3 a)-c), would yield the desired electrical properties. This process was performed on CNT arrays synthesized on Si-wafers approx. 46 *mm* wide and lengths between 25 *mm* and 150 *mm*.

Using a piece of fiber reinforced Teflon (Guaranteed NonPorous Teflon, GNPT), the vertical arrays of CNTs were knocked down and compressed onto the Si-wafer using a steel tool with small radius. The CNTs then formed a mechanically coherent piece of material with the CNTs aligned in the plane of the Si-wafer. Figure 4 a), and b) show the change of morphology of a small sample produced using this method.

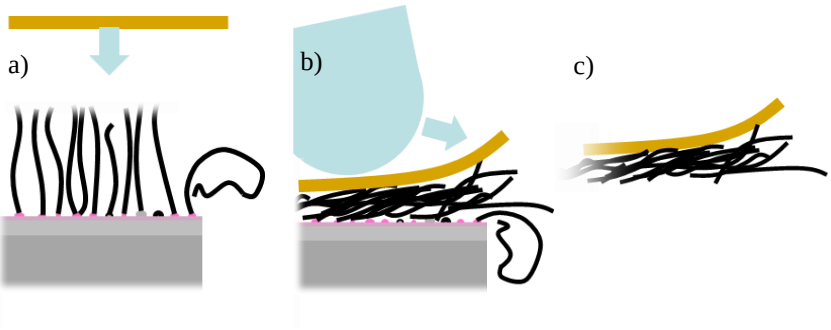

Figure 3: Knocked-down nanostitch fabrication: a-c) Schematic of the knock down procedure consisting of applying the Teflon sheet, compressive shear densification, and lift off of the densified CNT array.

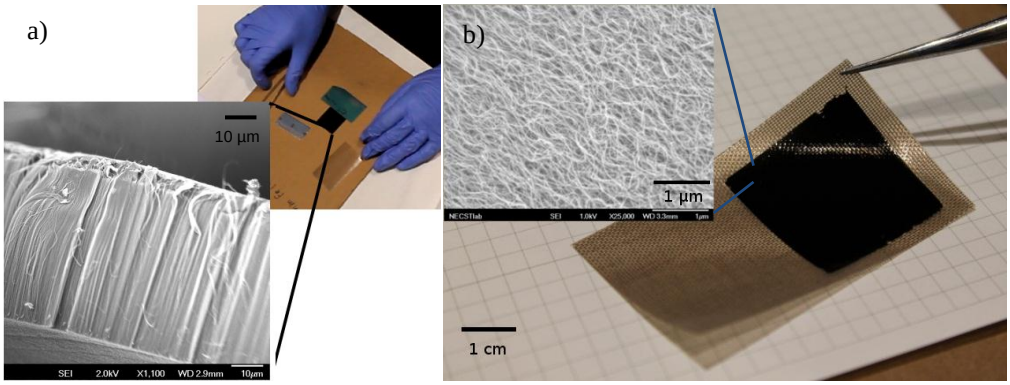

Figure 4: Fabricated knocked-down nanostitch: a) Scanning electron microscopy image illustrating the morphology of a vertically aligned array of CNTs after synthesis and before densification. The height of the shown array is shorter than the material used in the device, which was between 80 *µm* and 100 *µm* CNT lengths. b) Scanning electron microscopy image showing the morphology of a knocked-down nanostitch layer (inset) and optical image of a small patch on Teflon sheet.

The morphology of CNT arrays and patches at every scale from nano- to macroscopic determines the resulting properties. The most strongly effected properties are the transport properties, such as heat and electron transport, which are easily influenced by nanoscale structure and morphology changes. As the electrons can travel through the CNTs with relative ease, they encounter the largest barriers at the interfaces between the CNTs in an array, or at the interface between adjoining regions of CNT arrays. At these locations, tunneling is the dominant charge transport mechanism, which can be observed on a macroscopic level as a large electrical resistance[20]. This transport mechanism dissipates electrical power in form of heat. During the manufacturing of small area test samples, similar to the one seen in Figure 2 b), the resistance was monitored throughout the manufacturing process. Some constitutive morphological parameters of the CNT arrays are given in[14,21] which are also relevant to the synthesis process used in this report. Macroscopic features that cause heat or electrical flow barriers can influence the temperature distribution as well. Whenever electric pathways are constricted, local temperature gradients may arise.

IV. IPS Assembly and Testing

After the preliminary tests were performed, a larger number of CNTs arrays were placed adjacent to one another on an epoxy film and monitored electrically, through the various steps of curing the IPS nanocomposite layer onto the (pre-cured) aerosurface substrate (see Figure 4). The lay-up inside the bag consisted of a simple vacuum spreader on the inside of the aerosurface, and a soft silicone mat to prevent the vacuum bagging imprinting on the IPS layers. GNPT was placed under the silicone with the on the epoxy film, which encapsulated the CNTs during

the cure process. The electrical resistance was found to be extremely stable after a vacuum cure of 2 h at 120°*C* and 85 kPa pressure. Using temporary electrodes, heating tests could be performed successfully, even above the original curing temperature (see Figure 4c). Shortly before the actual wind tunnel test, the electrical connection was established using rivets through the entire aerosurface, which was also be used to affix the part to its support. Two separate icing protection devices were installed on the aerosurface (see Fig. 5a).

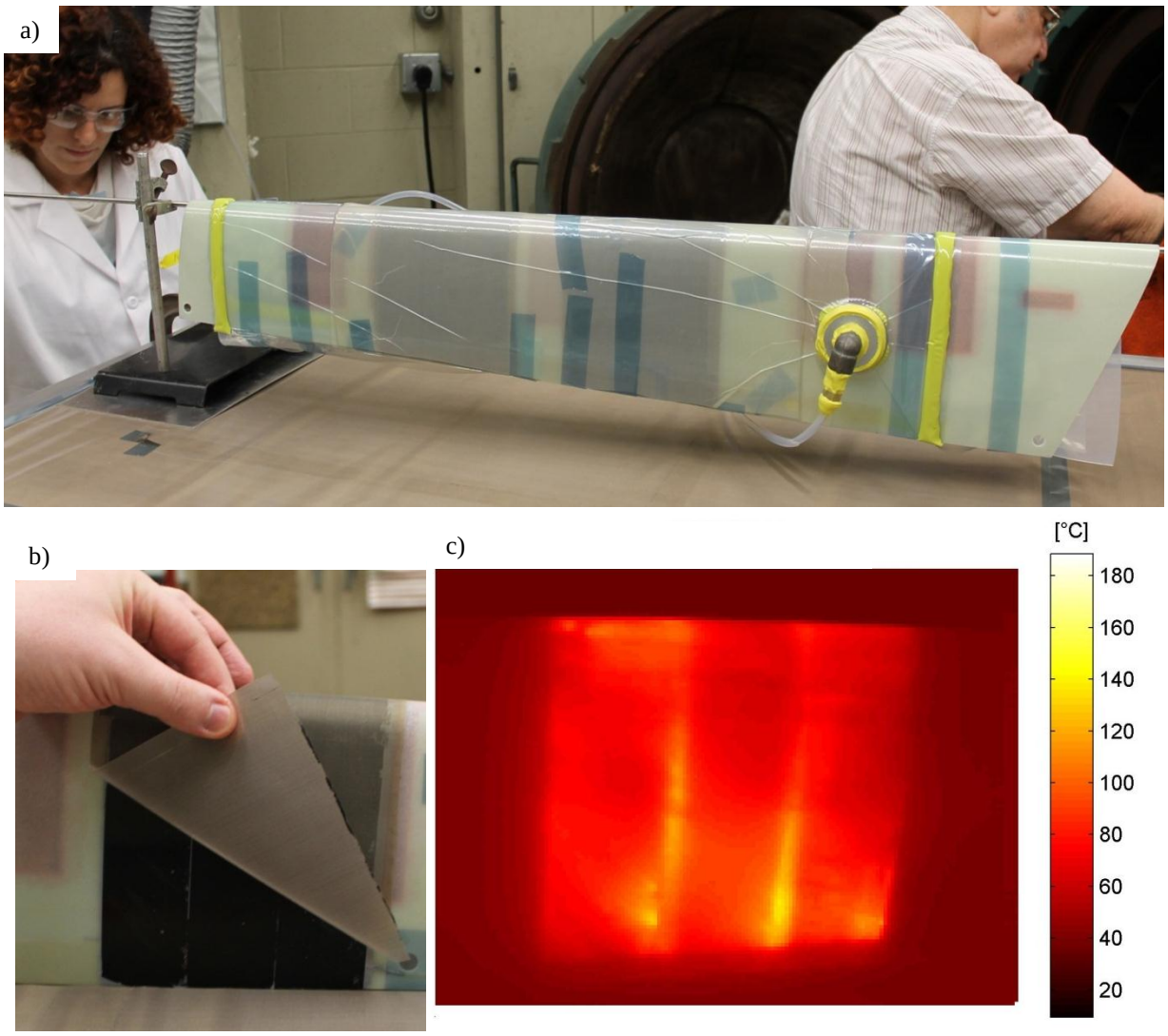

Fig. 5: IPS integration on aerosurface: a) The assembly in a vacuum bag just prior to curing. b) Unpacking the nanostitched IPS after successful cure. c) Thermal image of a preliminary heating experiment.

The ice tunnel test was performed at Cox & Company, Inc., New York, NY using -5°*F* to +25°*F* (-20.9°*C* to -3.9°*C*) with an airspeed of approx. 125 *mph* (55.9 *m/s*) and 1.1 g/m³ water content of 30 μ*m* mean volume droplet size. The peak power used in this experiment was approx. 8 kW/m², but generally 1 kW/m² was sufficient for anti-icing in the less harsh conditions. It should be noted that laboratory (not ice tunnel) experiments were performed to 40 kW/m^2, limited only by the power supply hardware. Figure 6 (top) shows the ice accretion typically observed after a few minutes exposure to the above icing conditions. Figure 6 (bottom left) illustrates the successful de-icing of glaze ice using a moderate power density. Figure 6 (bottom right) shows successful anti-icing.

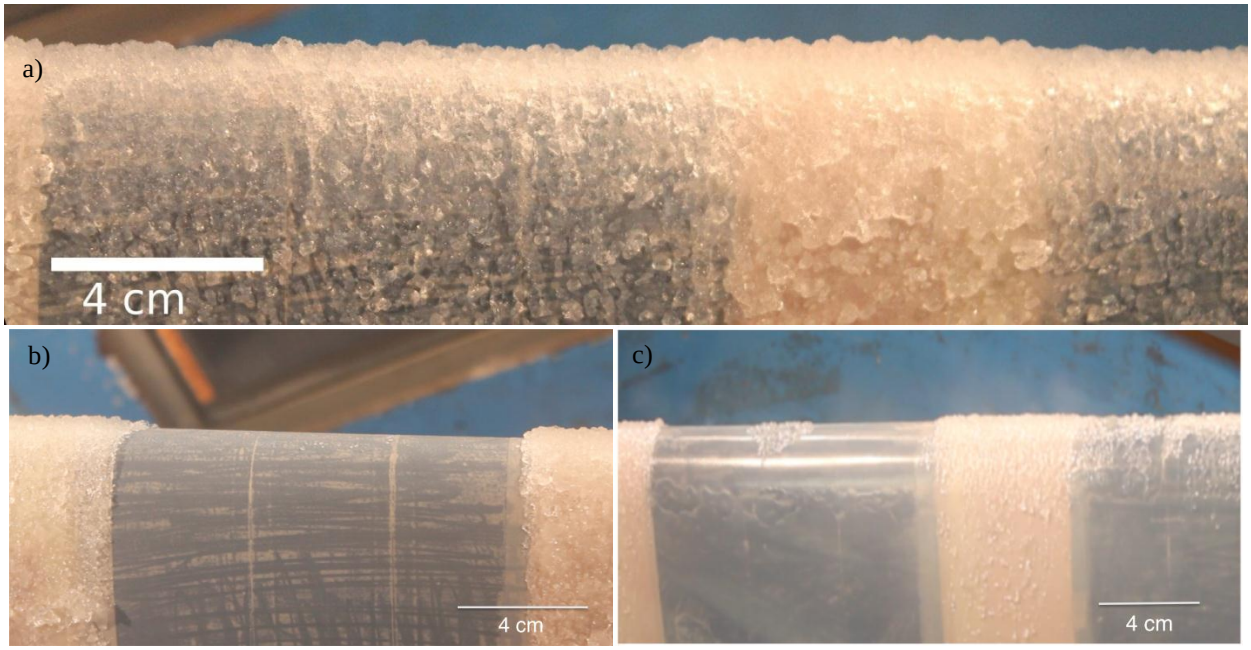

Fig. 6: Optical images from IPS testing in ice tunnel: a) Representative ice accretion after a few minutes of undisturbed exposure with deactivated electrothermal device. b) Aerosurface after successful de-icing. c) Aerosurface during anti-icing.

In light of this initial success of this prototype, which was not yet optimized in a number of ways, another experiment was recently performed that improved upon these results in several ways, such as controlled ice shedding. A particular feature of IPS that was explored in more detail is observed in Figure 6 where some bridging ice structures can be seen, which can easily form on fixed aerosurfaces and often significantly hinders ice shedding through a complex interplay of aerodynamics, water flowing towards the leading edge, among other factors. These problems were addressed by simply manufacturing an IPS of larger dimensions which also showed that the IPS can be manufactured in a co-curing process. Despite these demonstrations, there is still great potential for more powerful and efficient ice protection systems to be realized using the aforementioned design variables. Different systems made using these variables could be combined for de-icing, anti-icing, or other icing mitigation devices. Furthermore the versatility, potential sensor capabilities (ice detection), and minimally negative (and in some cases likely positive) effects on the mechanical properties from the nanostitch IPS merit continued investigation.

Acknowledgments

The authors would like to acknowledge financial support from NAVAIR SBIR contract N68335-11-C-0424, J. Gavin acknowledges support from the CMSE Research Experience for Undergraduates Program, as part of the MRSEC Program of the National Science Foundation under grant number DMR-0819762. Materials developed for use in this work were supported by Boeing, EADS, Embraer, Lockheed Martin, Saab AB, Composite Systems Technology, Hexcel, and TohoTenax through MIT's Nano-Engineered Composite aerospace STructures (NECST) Consortium. The authors would like to thank Richard Li (MIT), Itai Y. Stein (MIT), and John Kane (MIT) and the entire necstlab at MIT for technical support and advice. This work made use of the core facilities at the Institute for Soldier Nanotechnologies at MIT, supported by the U.S. Army Research Office under contract W911NF-07-D-0004, the Undergraduate Teaching Laboratory in the Department of Materials Science and Engineering at MIT, and the Shared Experimental Facilities supported in part by the MRSEC Program of the National Science Foundation under award number DMR-0819762.

References

[1] Chou T, Gao L, Thostenson ET, Zhang Z, Byun J., "An assessment of the science and technology of carbon nanotube-based fibers and composites", *Composites Science and Technology* 2010; pp. 1.

[2] Li C, Thostenson ET, Chou T., "Sensors and actuators based on carbon nanotubes and their composites: A review", *Composites Science and Technology*, 2008; pp. 1227.

[3] Al-Khalil, K.M., Ferguson, T.F.W.,Cox & Company, Inc., New York, NY, "Hybrid Ice Protection System for use on Roughness-Sensitive Airfoils", Patent No. US 6 196 500 B1, filed 11 June 1999.

[4] Z. Goraj, , "An Overview of the Deicing and Antiicing Technologies with Prospects for the Future", *24th International Congress of the Aeronautical Sciences*, 29 August - 3 September 2004, Yokohama, Japan.

[5] Blanco J, Garcia EJ, Guzman de Villoria R, Wardle BL, "Limiting Mechanisms of Mode I Interlaminar Toughening of Composites Reinforced with Aligned Carbon Nanotubes", *Journal of Composite Materials*, 2009; pp. 825.

[6] Strehlow, R. H.; Moser, R., "Capitalizing on the Increased Flexibility that Comes from High Power Density Electrothermal Deicing", *USA SAE International*, Warrendale, PA 2009.

[7] Jorio, A.; Dresselhaus, G.; Dresselhaus, M. S., „Carbon nanotubes. "Advanced topics in the synthesis, structure, properties and applications", *Topics in applied physics*, Berlin: Springer-Verlag, 2008, ISBN: 978-3-540-72864-1

[8] Garcia, E.J., Wardle, B.L., and A.J. Hart, "Joining Prepreg Composite Interfaces with Aligned Carbon Nanotubes",*Composites Part A*, Vol. 39, 2008, pp. 1065.

[9] Guzmán de Villoria, R., Ydrefors, L., Hallander, P., Ishiguro, K., Nordin, P., and B.L. Wardle, "Aligned Carbon Nanotube Reinforcement of Aerospace Carbon Fiber Composites: Substructural Strength Evaluation for Aerostructure Applications", AIAA-2012-1220149,*53rd AIAA Structures, Structural Dynamics, and Materials (SDM) Conference*, 23-26 April, 2012, Honolulu, HI, USA.

[10] Nirmalraj P.N., Lyons P.E., De S, Coleman J.N., Boland J.J.,"Electrical Connectivity in Single-Walled Carbon Nanotube Networks". *Nano Letters*, 2009, pp. 3890.

[11] Nirmalraj P.N., Bellew A.T., Bell A.P., Fairfield J.A., McCarthy E.K., O'Kelly C. et al,"Manipulating Connectivity and Electrical Conductivity in Metallic Nanowire Networks", *Nano Letters* 2012; pp. 5966.

[12] Stein IY, Wardle BL. "Coordination number model to quantify packing morphology of aligned nanowire arrays". *Phys. Chem. Chem. Phys*, 2013; pp. 4033.

[13] Fisher FT, Bradshaw RD, Brinson LC, "Effects of nanotube waviness on the modulus of nanotube-reinforced polymers", *Appl. Phys. Lett*, 2002, pp. 4647.

[14] Cebeci, H., Guzman de Villoria, R., Hart, A. J., Wardle, B. L., "Multifunctional properties of high volume fraction aligned carbon nanotube polymer composites with controlled morphology", *Composites Science and Technology*, 2009, pp. 2649.

[15] Tawfick S, O'Brien K, Hart AJ. "Flexible High-Conductivity Carbon-Nanotube Interconnects Made by Rolling and Printing", *Small*, 2009; pp. 2467.

[16] Bradford PD, Wang X, Zhao H, Maria J, Jia Q, Zhu Y., "A novel approach to fabricate high volume fraction nanocomposites with long aligned carbon nanotubes", *Composites Science and Technology* 2010; pp. 1980.

[17] Jiang Y, Lin L. "A two-stage, self-aligned vertical densification process for as-grown CNT forests in supercapacitor applications", *Sensors and Actuators A: Physical*, 2012, pp. 261.

[18] Pint CL, Xu Y, Pasquali M, Hauge RH. "Formation of Highly Dense Aligned Ribbons and Transparent Films of Single-Walled Carbon Nanotubes Directly from Carpets", *ACS Nano*, 2008, pp. 1871–8.

[19] García EJ, Hart AJ, Wardle BL, Slocum AH. Fabrication and Nanocompression Testing of Aligned Carbon-Nanotube–Polymer Nanocomposites. Adv. Mater. 2007;19(16):2151–6.

[20] Li C, Thostenson ET, Chou T., "Dominant role of tunneling resistance in the electrical conductivity of carbon nanotube–based composites". *Appl. Phys. Lett*, 2007, pp. 223114.

[21] S. Wicks, R. Guzman de Villoria, and B. L. Wardle, "Interlaminar and Intralaminar Reinforcement of Composite Laminates with Aligned Carbon Nanotubes", *Composite Science and Technology*, 2010, pp. 20.